A New 18-Pulse AC-DC Converter with Regulated DC Output and High Power Factor for Three-Phase Applications

Falcondes José Mendes de Seixas (*) and Ivo Barbi

Federal University of Santa Catarina – Department of Electrical Engineering
Power Electronics Institute – http://www.inep.ufsc.br
88040-970 - P.O. Box 5119 –- Florianópolis – SC – Brazil
Phone: +55-48-331-9204 - fax: +55-48-234-5422 - falcon@inep.ufsc.br
(*) Is with the UNESP - São Paulo State University – http://www.dee.feis.unesp.br

***Abstract* – This work presents a new 12kW high power factor three-phase rectifier based on a Y-connected differential autotransformer with reduced kVA and 18-pulse input current followed by three DC-DC boost converters. The topology provides a regulated output voltage and natural three-phase input power factor correction. The lowest input current harmonic components are the 17th and the 19th. Three boost converters, with constant input currents and regulated parallel connected output voltages are used to process 4kW each one.**

Analytical results from Fourier analyses of winding currents and the vector diagram of winding voltages are presented. Experimental results to verify the proposed concept is shown in the paper.

I. Introduction

In telecommunication systems, conventional input stage of power supplies is widely realized as voltage DC-link converters. In many cases, the AC supply voltage is connected to a DC link voltage by a diode rectifier with output filter capacitor. A high-frequency DC-DC converter, with regulated output voltage, is then connected in series with the DC-link voltage.

Motivated by high efficiency, high power density, low cost and robustness, an uncontrolled three-phase bridge directly connected to the AC supply has been used. However, this concept shows, as disadvantage, high low-frequency current harmonics, due to the output capacitor, which leads to a distortion of the AC supply voltage.

Various international standards like IEEE-519 and IEC-1000-3-2, were proposed to maintain the THD (Total Harmonic Distortion) and the Power Factor (PF) at acceptable levels. This is especially important for guaranteeing universal applicability of telecommunication rectifiers.

Furthermore, the conventional power supplies are being replaced more and more by three-phase modular rectifier systems, due to the advantages of the latter concerning operational behavior, system technology, and costs [01].

In the same way that the great number of works developed for power factor correction in single-phase systems, the techniques for three phase systems to operate with power factor correction are growing, either through converters with one or more associated switches, or by using specially connected transformers. In general, the techniques that use transformers or mixed systems, with transformers and static converters, operate well in higher power systems [02,03].

A parallel connection of three six-pulse bridge rectifier is used to obtain 18-pulse uncontrolled converter. Usually, an Interphase Transformer (IPT) connected on the DC sides of the three bridge rectifiers is required to absorb the instantaneous voltage differences between the bridges. When a non-isolated transformer is used, two IPT are needed: one connected to the positive outputs, and another connected to the negative outputs. The size, the loss and the cost of the IPT are, therefore, increased.

Figure 1 shows the basic diagram for a non-isolated 18-pulse converter using two conventional IPT to improve parallel connection on the DC sides.

This work proposes a new 18-pulse converter using a Y-connected differential autotransformer. The autotransformer is designed to feed three six-pulse bridge rectifiers displaced in phase by 20°. The autotransformer power rate is only 22% of the output kVA and the lowest order harmonics are the 17th and the 19th.

In order to provide parallel-connected [04] and regulated output voltages, without an IPT, three boost converters with additional diodes were proposed.

Six small size high-frequency boost inductors, as shown in figure 2, replace the large interphase transformers. The continuous conduction mode and output regulated voltage are guaranteed by basic and simple control strategy of the boost converter. The inductor currents of each converter are kept constant with a little high frequency ripple.

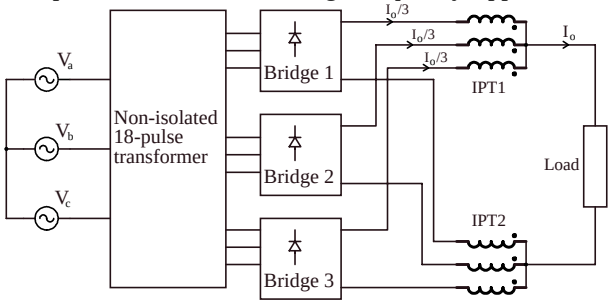

Fig. 1. 18-Pulse converter with conventional IPT

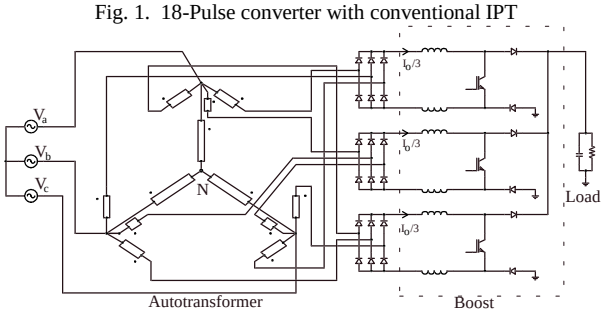

Fig. 2. Proposed topology of the 18-pulse regulated boost converter

Each boost converter is studied separately and a simple passive lossless snubber circuit [05] is applied to reduce the over-current through the switch and the losses, during the diode reverse recovery. This snubber circuit provides a good turn-on transition for the switch.

Experimental results with relevant waveforms to verify the power factor and details of switch commutation are presented.

II. Analysis of the Proposed 18-Pulse Y-Connected Differential Autotransformer

To simplify the analyses of the autotransformer, the boost converters are eliminated and, furthermore, three independent inductive loads, at the same values, are connected on the DC sides of the bridge rectifiers, as shown in figure 3. The main equations and relationships of winding voltages and currents are studied.

The autotransformer is supplied by a three-phase balanced voltage system. The output voltages are composed by three rectifier systems of three-phase voltages, also balanced. One of these systems is placed in the same phase of the supply voltage and the others are placed of $+20^o$ and -20°, with regard to the supply system.

The 18-pulse converter is obtained when each output voltage system is connected to a six-pulse diode rectifier. Three identical loads with current source characteristic are used.

A. Vector Diagram of the Autotransformer Winding Voltages

The three secondary voltage systems are obtained by the combination of ratios between primary and secondary windings. The vector diagram used to obtain all voltage system is shown in figure 4.

The primary windings of the autotransformer are formed by L_a, L_b and L_c, Y-connected and linked to the line voltages V_a, V_b and V_c. In this connection, a virtual neutral point N is generated.

The secondary windings are designed, in such way that, the turns ratio and the connection between them and the primary winding generate three different three-phase systems with 20° phase-shift from each other. These voltages feed the rectifiers.

All the windings of L_a, L_{an}, L_{a1} and L_{a2} are coupled together in the same limb core, the resulting voltages V_a, V_{an}, V_{a1} and V_{a2} are in phase. The same applies to phases "b" and "c", as shown in figure 4.

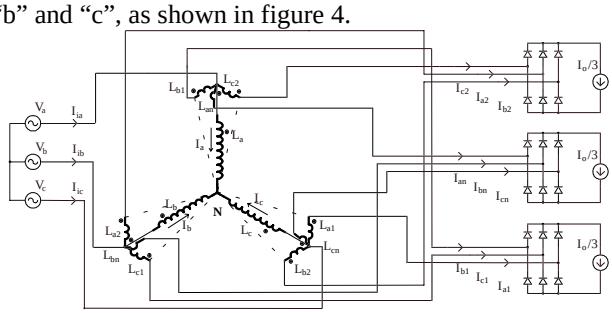

Fig. 3. A simplified circuit of proposed topology for analysis

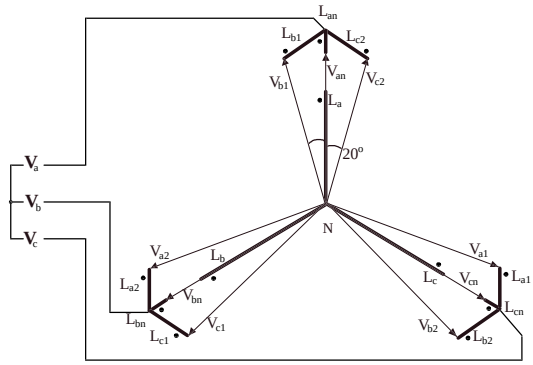

Fig. 4. Vector diagram

The magnitude of the voltages across the secondary windings, is obtained as follows.

$$V_{Lb1} = V_{Lc2} = V_a . \frac{\sin(20^o)}{\sin(100^o)} = 0.3473 \,.\, V_a \qquad (01)$$

$$V_{Lc1} = V_{La2} = V_b . \frac{\sin(20^o)}{\sin(100^o)} = 0.3473 \,.\, V_b \qquad (02)$$

$$V_{La1} = V_{Lb2} = V_c . \frac{\sin(20^o)}{\sin(100^o)} = 0.3473 \,.\, V_c \qquad (03)$$

The winding turns-ratio (n_2) that ensure a displacement of 20° is given by (04).

$$n_2 = \frac{V_a}{V_{Lb1}} = \frac{V_a}{0.3473 \,.\, V_a} = 2.88 \qquad (04)$$

This result shows that the secondary turns are 2.88 times lower than the primary turns.

The magnitude voltages between each secondary terminal with respect to the virtual neutral point N are obtained as follows.

$$V_{b1} = V_{c2} = V_a . \frac{\sin(60^o)}{\sin(100^o)} = 0.8794 \,.\, V_a \qquad (05)$$

$$V_{c1} = V_{a2} = V_b . \frac{\sin(60^o)}{\sin(100^o)} = 0.8794 \,.\, V_b \qquad (06)$$

$$V_{a1} = V_{b2} = V_c . \frac{\sin(60^o)}{\sin(100^o)} = 0.8794 \,.\, V_c \qquad (07)$$

We can observe that the voltage magnitudes of each three-phase system are about 88% reduced in comparison input phase voltages.

The third secondary three-phase voltage system is in phase with the primary one. Its voltages however, must be in agreement with the others secondaries. So, the following equations must be fulfilled:

$$V_{Lan} = V_a - 0.8794 \,.\, V_a = 0.1206 \,.\, V_a \qquad (08)$$

$$V_{Lbn} = V_b - 0.8794 \,.\, V_b = 0.1206 \,.\, V_b \qquad (09)$$

$$V_{Lcn} = V_c - 0.8794 \,.\, V_c = 0.1206 \,.\, V_c \qquad (10)$$

Were, V_{Lan}, V_{Lbn} and V_{Lcn} are the magnitude of the voltages across the secondary windings L_{an}, L_{bn} and L_{cn}, respectively.

The winding turns-ratio to ensure 88% from primary voltage (n_1), without displacement, is given by.

$$n_1 = \frac{V_a}{V_{Lan}} = \frac{1}{0.1206} = 8.29 \qquad (11)$$

This result shows that this secondary turns is 8.29 times lower than the primary turns.

The magnitude voltages for these secondary terminals, with respect to the virtual neutral point N, are obtained as follows.

$$V_{an} = 0.8794 \,.\, V_a \tag{12}$$

$$V_{bn} = 0.8794 \,.\, V_b \tag{13}$$

$$V_{cn} = 0.8794 \,.\, V_c \tag{14}$$

B. Analysis of the Winding Currents

The technique to eliminate harmonic of current in the multiple pulse converters requires current-mode operation to the load.

In this case, the 18-pulse converter, formed by three-bridge rectifier, each converter conducts 1/3 of the load current ($I_o/3$). The currents in the secondary windings are the same to the input currents of each bridge.

The waveform of the input V_a and the current through one secondary winding (L_{an}) are shown in figure 5. These waveforms are adopted as angular reference to represent the other ones.

The waveform of Ian can be decomposed in *Fourier series* by the conventional way. By the way, when discontinuous function is considered, the series terms can be obtained by inspection. We can observe that this waveform presents alternate symmetry, the negative half cycle is an inverted reproduction of the positive half cycle. Thus, the even harmonic are zero and there are not terms in cosines. The average value is also zero.

We can observed that this winding (L_{an}) conducts the current $I_o/3$ during 120° ($2\pi/3$), starting from 30° ($\pi/6$). Thus, for k=1, 3, 5, ...,the expression of the current results:

$$I_{an}(t) = \frac{4}{\pi}.\frac{I_o}{3}.\sum_k \frac{1}{k}.\cos\left(k.\frac{1}{6}\right)\sin(k.\omega t) \tag{15}$$

The waveforms of all currents through the secondary windings are the same, only with a 20° phase-shift among each three-phase system. The other currents are represented by the same equation of Ian as shown below. Therefore, all phases are adjusted.

$$I_{bn}(t) = \frac{4}{\pi}.\frac{I_o}{3}.\sum_k \frac{1}{k}.\cos\left(k.\frac{1}{6}\right)\sin\left[k.\left(\omega t + \frac{2\pi}{3}\right)\right] \tag{16}$$

$$I_{cn}(t) = \frac{4}{\pi}.\frac{I_o}{3}.\sum_k \frac{1}{k}.\cos\left(k.\frac{1}{6}\right)\sin\left[k.\left(\omega t - \frac{2\pi}{3}\right)\right] \tag{17}$$

In the other secondary three-phase system, the currents are expressed by:

$$I_{a1}(t) = \frac{4}{\pi}.\frac{I_o}{3}.\sum_k \frac{1}{k}.\cos\left(k.\frac{1}{6}\right)\sin\left[k.\left(\omega t - \frac{100\pi}{180}\right)\right] \tag{18}$$

$$I_{b1}(t) = \frac{4}{\pi}.\frac{I_o}{3}.\sum_k \frac{1}{k}.\cos\left(k.\frac{1}{6}\right)\sin\left[k.\left(\omega t + \frac{20\pi}{180}\right)\right] \tag{19}$$

$$I_{c1}(t) = \frac{4}{\pi}.\frac{I_o}{3}.\sum_k \frac{1}{k}.\cos\left(k.\frac{1}{6}\right)\sin\left[k.\left(\omega t + \frac{140\pi}{180}\right)\right] \tag{20}$$

To the last system, the currents are expressed by:

$$I_{a2}(t) = \frac{4}{\pi}.\frac{I_o}{3}.\sum_k \frac{1}{k}.\cos\left(k.\frac{1}{6}\right)\sin\left[k.\left(\omega t + \frac{100\pi}{180}\right)\right] \tag{21}$$

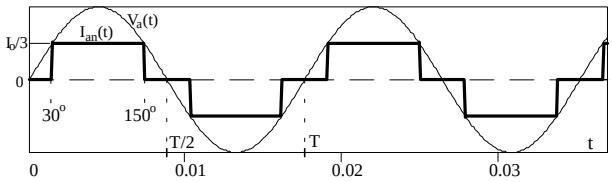

Fig. 5. Primary reference voltage and secondary current to phase indexed by "a"

$$I_{b2}(t) = \frac{4}{\pi}.\frac{I_o}{3}.\sum_k \frac{1}{k}.\cos\left(k.\frac{1}{6}\right)\sin\left[k.\left(\omega t - \frac{140\pi}{180}\right)\right] \tag{22}$$

$$I_{c2}(t) = \frac{4}{\pi}.\frac{I_o}{3}.\sum_k \frac{1}{k}.\cos\left(k.\frac{1}{6}\right)\sin\left[k.\left(\omega t - \frac{20\pi}{180}\right)\right] \tag{23}$$

The primary winding currents (I_a, I_b and I_c) can be obtained by considering the currents of the three secondary winding coupled to the same limb core and by turns-ratio (n_1=8.29 and n_2=2.88). As mentioned bottom, winding with the same index (a, b or c) are coupled in the same limb.

$$I_a(t) = \left(\frac{I_{a1}(t) + I_{a2}(t)}{n_2} - \frac{I_{an}(t)}{n_1}\right) \tag{24}$$

$$I_b(t) = \left(\frac{I_{b1}(t) + I_{b2}(t)}{n_2} - \frac{I_{bn}(t)}{n_1}\right) \tag{25}$$

$$I_c(t) = \left(\frac{I_{c1}(t) + I_{c2}(t)}{n_2} - \frac{I_{cn}(t)}{n_1}\right) \tag{26}$$

Figure 6 shows the primary current (I_a). It is obtained by composition of equation (24) from (04), (11), (15), (18) and (21). This solution is easily found and plotted through *MathCad* program.

C. Analysis of the Line-Input Currents

The input currents I_{ia}, I_{ib} and I_{ic} are obtained by summing all currents through windings at same node as shown in figure 3. So, the follow equations can be written.

$$I_{ia}(t) = I_a(t) + I_{an}(t) + I_{b1}(t) + I_{c2}(t) \tag{27}$$

$$I_{ib}(t) = I_b(t) + I_{bn}(t) + I_{c1}(t) + I_{a2}(t) \tag{28}$$

$$I_{ic}(t) = I_c(t) + I_{cn}(t) + I_{a1}(t) + I_{b2}(t) \tag{29}$$

Figure 7 shows the phase currents that are obtained by composition of equation (27) to (29) from (15) to (26).

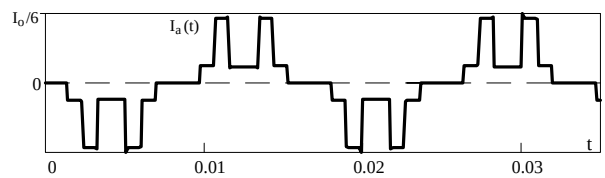

Fig. 6. Primary current waveform

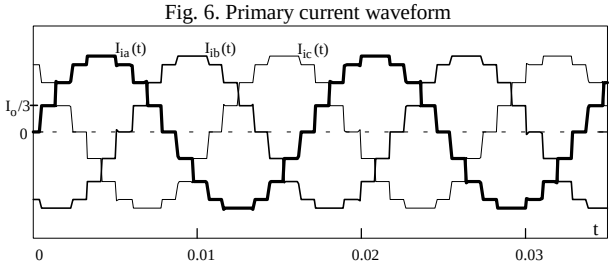

Fig. 7. Three-phase input currents

D. Harmonic Analysis for Input Phase Current

Total Harmonic Distortion (THD) is calculated by relationship between rms values of the fundamental components and all phase current harmonics. In these calculations *MathCad* program has considered the first 1000 harmonic components (k=1,3,5 ...999).

The total rms value for all harmonics of the phase current I_{ia} and the rms current for fundamental component I_{ia1} (for k=1), are calculated through (30) and (31):

$$I_{ia} = \sqrt{\frac{1}{2\pi}.\int_0^{2\pi} I_{ia}(t)^2.d\omega t} \qquad (30)$$

$$I_{ia1} = \sqrt{\frac{1}{2\pi}.\int_0^{2\pi} I_{ia1}(t)^2.d\omega t} \qquad (31)$$

Where, $I_{ia}(t)$ is solved by (27) for k=1,3,5,... and $I_{ia1}(t)$ is solved by (27) for k=1.

From (30) and (31), the THD is easily obtained by (32).

$$THD = \sqrt{\frac{I_{ia}^2 - I_{ia1}^2}{I_{ia1}^2}} = 10.7\% \qquad (32)$$

The Power Factor (PF) is calculated by (33). The displacement between the phase current and the phase voltage is negligible.

$$PF = \frac{1}{\sqrt{1+THD^2}} = 0.994 \qquad (33)$$

Figure 8 shows the frequency spectrum of the input phase current $I_{ia}(t)$. We can observe that 18-pulse converter presents only harmonic orders X.(18±1), for X=1,2,3,.... The lowest harmonic orders are the 17th and the 19th.

E. Power Rate of the Autotransformer

The shape of all secondary winding currents are equal, but each one is shifted in phase to generate the three-phase systems. Anyway, all rms value of secondary currents are the same. Then, they can be calculated through (34).

$$I_{an} = I_o.\sqrt{\frac{1}{2\pi}.\int_0^{2\pi} \frac{I_{an}(t)^2}{I_o}.d\omega t} \qquad I_{an} = 0.272 \,.\, I_o \qquad (34)$$

The primary winding currents have the same rms value and can be expressed by (35).

$$I_a = I_o.\sqrt{\frac{1}{2\pi}.\int_0^{2\pi} \frac{I_a(t)^2}{I_o}.d\omega t} \qquad I_a = 0.078 \,.\, I_o \qquad (35)$$

Where, $I_{an}(t)$ and $I_a(t)$ are the secondary and the primary winding currents, respectively. Other currents are calculated with the same way.

The voltage across secondary windings with the same phase than primary ones, L_{an}, L_{bn} and L_{cn}, are reduced by turns ratio n_1. Therefore, the relationship between these voltages is expressed for (08) to (10).

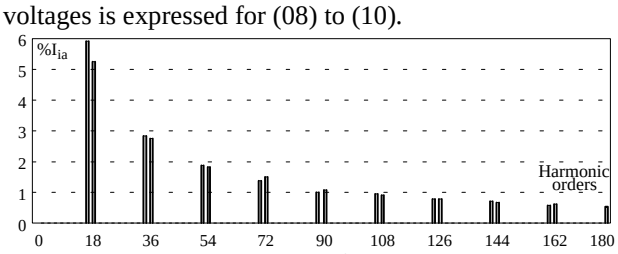

Fig. 8. Frequency spectrum for input phase currents

The voltage across secondary windings with phase shift of 20° in relation to primary ones, L_{a1}, L_{a2}, L_{b1}, L_{b2}, L_{c1} and L_{c2}, are reduced by turns ratio n_2. Therefore, the relationship between these voltages are expressed for (01), (02) and (03).

Expression (36) and (37) give the average voltage from output of the rectifier.

$$V_o = \frac{6}{2\pi}.\int_0^{2\pi}\left(\sqrt{2}\sqrt{3}.0.8794.V_a.\sin(\omega t)\right)d\omega t \qquad (36)$$

$$V_o = 2.057 \,.\, V_a \qquad (37)$$

The secondary power rate VA is obtained by summing of the product of voltage and current of each secondary winding, as shown in (38).

$$S_2 = 0.323 \,.\, P_o \qquad (38)$$

The primary power rate VA is obtained by summing of the product of voltage and current of each primary winding, as shown in (39).

$$S_1 = 0.114 \,.\, P_o \qquad (39)$$

Where

$$P_o = V_o \,.\, I_o \qquad (40)$$

Thus, the autotransformer power rate is given by average value between S1 and S2. Then,

$$S = 0.218 \,.\, P_o \qquad (41)$$

III. Proposed Boost Converter Strategy

The boost converter is chosen because it provides a simple regulated output voltage and regulated inductor current. Furthermore, it is very easy to obtain three parallel connected boost converters [04], as shown in figure 2.

The conventional boost converter can not be used because when two or more switches are closed, the current flowing through the first boost returns through the second one. One diode that is added in the conventional boost can solve this problem.

Another problem occurs when all switches are simultaneously open. The current flows through the first boost, through the load and returns through the second one. This problem is solved by division of each boost inductor in two series connected inductors, as shown in figure 2. After the switch turn-off, the lower inductor forces the current from upper one to comes back through it. In this way, the lower inductors are necessary.

This connection is very important to the operating of the circuit. It improves an independent operation mode among the boost converters.

A. Command Circuit for Regulated Boost Converter

To improve regulated current in boost inductor and regulated output voltage, various command circuits such as constant hysteresis and average current-mode control were investigated. The simplest strategy to promote both regulated voltage and regulated current is shown in block diagram in figure 9.

This is a conventional scheme to control each boost converter. The output voltage error amplifier is used as reference by the current regulator and the output current error amplifier is connected to PWM controller at constant

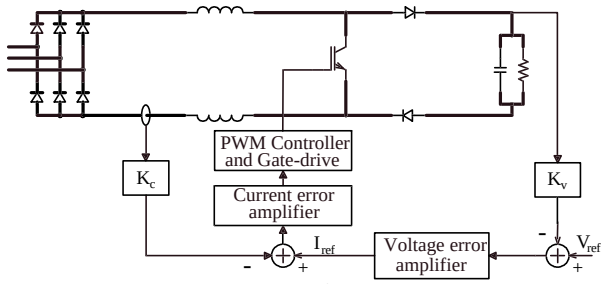

Fig. 9. Command strategy for one boost converter

frequency. Anyway, all boost converters operate independently and decoupled. Therefore, the synchronism among them is not necessary.

In order to connect all boost converters in parallel, only one voltage regulator is necessary. Fortunately, the command circuit becomes simpler, as shown in figure 10.

IV. Experimental Results

A prototype rated at 12kW, input line voltage equal to 380V and DC output voltage equal to 600V has been built and tested in the laboratory. The implemented circuit is shown in figure 10.

To reduce the stress current due the recovery diode and to reduce the turn-on losses on IGBT, a regenerative snubber circuit (L_s, D_{s1}, D_{s2} and C_s) [05] is used.

The more relevance components and the main specifications are reported as follows.

- Primary windings N(L_a, L_b, L_c) = 330 turns with 20AWG wire
- Secondary windings N(L_{an}, L_{bn}, L_{cn}) = 40 turns with 15AWG wire
- Secondary windings N(L_{a1}, L_{b1}, L_{c1}) = 114 turns with 15AWG wire
- Secondary windings N(L_{a2}, L_{b2}, L_{c2}) = 114 turns with 15AWG wire
- Central area of the "EI" three-Limb core = 27cm^2
- Three-phase bridge = SKD 30/08 A1 (Semikron)
- Active switch = IGBT (IRG4PC30W)
- Boost inductors = 1mH (60 turns on core E65-26)
- Boost diodes = HFA15TB60
- Snubber diodes = HFA15TB60
- Snubber inductor L_s = 2μH (4 turns on core E30-7)
- Snubber capacitor C_s = 47ηF
- Output capacitors C_o = 470 μF
- Current sensor = LA-25PN
- PWM circuit = LM 3524
- Operational amplifier = LM 324
- Optocoupler = HP 2211

Figure 11 shows a detail of the main switch turn-on transition with the snubber circuit installed.

Figure 12 shows the most important result of this work. It shows the waveforms for input current and input voltage in the same phase. We can observed the shape of input current between experimental result (fig. 12) and mathematical results (fig. 7) are the same. The input PF and the THD of the input current measured are equal to 0.99 and 8.8%, respectively.

Figure 13 shows the three currents displaced by 20° in phase. With this figure we can visualise one phase of each three-phase systems (I_{a1}, I_{an} and I_{a2}).

The boost inductor regulated currents are shown in figure 14.

Figure 15 shows the efficiency of the converter – boost, autotransformer and total.

V. Conclusion

In this paper we presented a three-phase high input power factor rectifier, intended to be used in the design of a 12kW rectifier unity for telecommunications.

The converter is composed of a 18-pulse rectifier based on a differential Y-connected autotransformer and three six-pulse diode bridge, and three boost DC-DC converters.

From the studies reported in this paper, we draw the conclusion as follows:

- ✓ The proposed circuit works according to the predicted models;

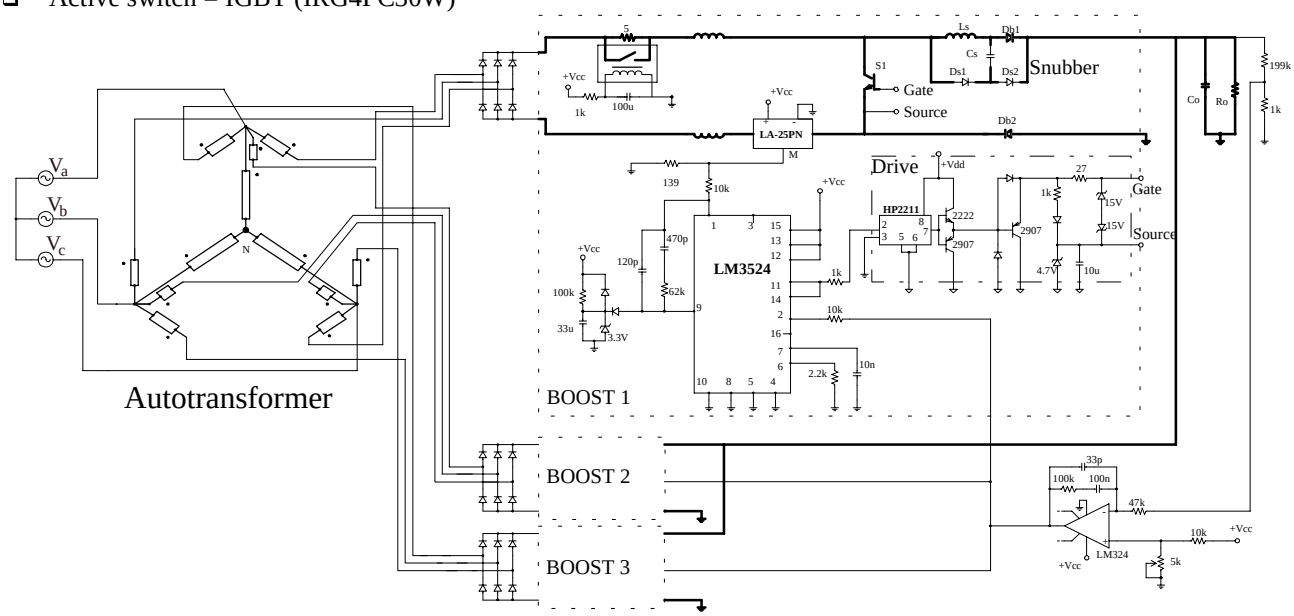

fig. 10. Complete implemented circuit

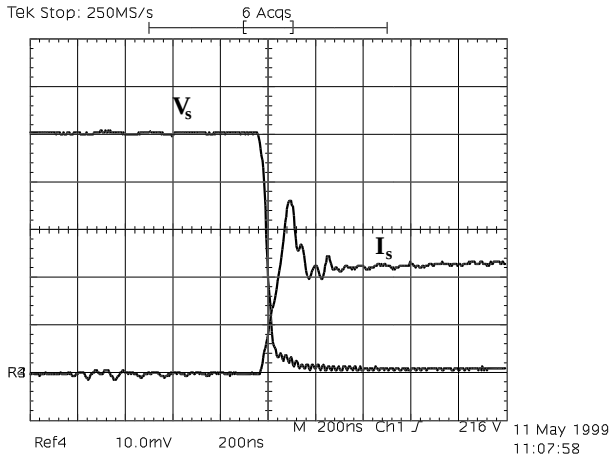

Fig. 11. Detail of the main switch turn-on transition
(200ηs/Div, 100V/Div, 5A/Div)

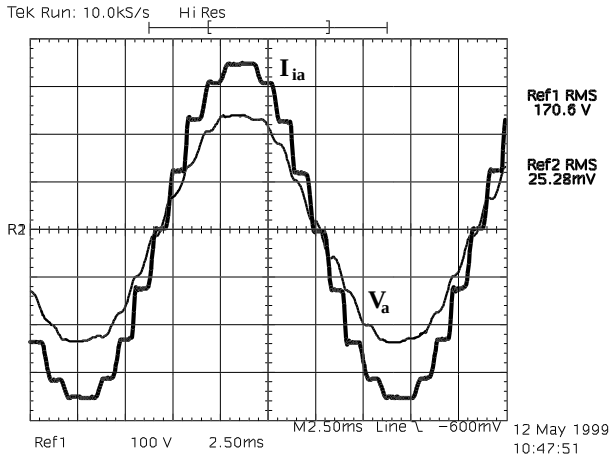

Figure 12: Input current and voltage
(2.5ms/Div, 100V/Div, 10A/Div)

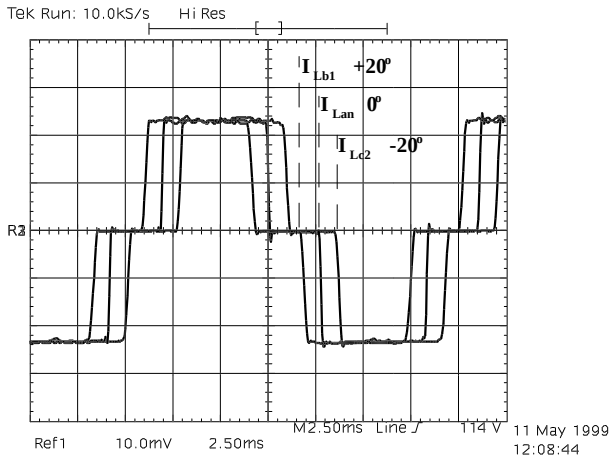

Fig. 13. Bridge input currents displaced by 20° in phase
(2.5ms/Div, 5A/Div)

- ✓ The input power factor and current THD are equal to 0.99 and 8.8%, respectively;
- ✓ The low frequency 18-pulse autotransformer is rated at 22% of the output power. Therefore, the weight and volume are compatible with the telecommunication power supply specifications.

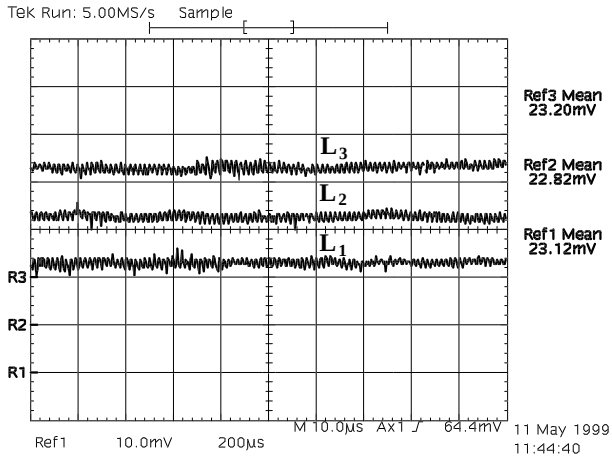

Fig. 14. Boost inductor currents
(200µs/Div, 5A/Div)

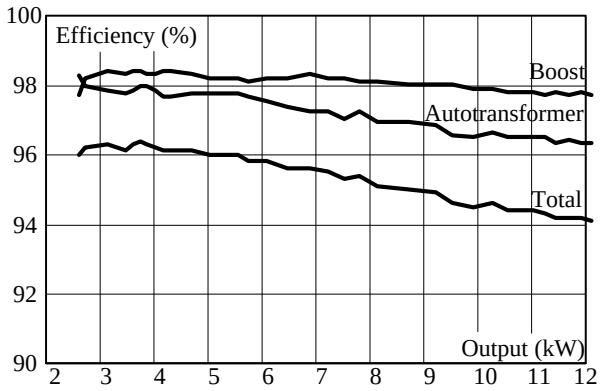

Fig. 15. Efficiency

- ✓ It employs three active switches that make this rectifier simpler and more reliable than the rectifier with six active switches.
- ✓ It is controlled by very simple PWM dedicated integrated circuit, not requiring multipliers.

It is the author's opinion that the proposed rectifier is a good candidate for 12 kW power supply design for telecommunications, with many advantages over the topologies presently being used in these applications.

VI. References

[01] J. W. Kolar, F. C. Zach "A Novel Three-Phase Utility Interface Minimizing Line Current Harmonics of High-Power Telecommunications Rectifier Modules", IEEE Trans. on Industrial Electronics, Vol. 44, pp. 456-467 Aug. 1997.

[02] Paice, Derek A. "Power Electronic Converter Harmonic Multipulse Methods for Clean Power", N.Y., IEEE Press, 1996.

[03] S. Choi, P. N. Enjeti, I. J. Pitel "Polyphase Transformer Arrangements with Reduced kVA Capacities for Harmonic Current Reduction in Rectifier-Type Utility Interface", IEEE Trans. on Power Electronics, Vol. 11, pp. 680-690, Set. 1996.

[04] G. Spiazzi, F. C. Lee "Implementation of Single-Phase Boost Power-Factor-Correction Circuits in Three-Phase Applications" IEEE Trans. on Industrial Electronics, Vol. 44, pp. 365-370 Jun. 1997.

[05] A. Pietkiewicz and D. Tollik "Snubber circuit and Mosfet Paralleling Considerations for High Power Boost-Based Power-Factor Correctors" Proceedings of INTELEC'95, pp. 41-45, 1995.